

MAGNETIC HYSTERESIS AND COMPLEX SUSCEPTIBILITY AS MEASURES OF  
AC LOSSES IN A MULTIFILAMENTARY NbTi SUPERCONDUCTOR

R. B. Goldfarb and A. F. Clark  
Electromagnetic Technology Division  
National Bureau of Standards  
Boulder, Colorado 80303

### Abstract

Magnetization and ac susceptibility of a standard NbTi superconductor were measured as a function of longitudinal dc magnetic field. The ac-field-amplitude and frequency dependences of the complex susceptibility are examined. The magnetization is related to the susceptibility by means of a theoretical derivation based on the field dependence of the critical current density. Hysteresis losses, obtained directly from dc hysteresis loops and derived theoretically from ac susceptibility and critical current density, were in reasonable agreement.

### Introduction

When subjected to alternating or transient magnetic fields, superconducting wires exhibit losses. These may be categorized into hysteresis losses, eddy-current losses, coupling losses, and self-field losses. Bulk hysteresis losses are frequency independent and arise mostly from flux pinning in the superconducting filaments. There may be, in addition, hysteretic losses due to pinning at the filament surface. At high frequencies, eddy-current losses occur within the matrix and on the wire surface (skin effect). Coupling losses in the matrix, important over about 1 kHz, are caused by the transfer of coupling currents between filaments. If there is a transport current, matrix eddy-current losses arise from the self field.

There are a few general methods of measuring ac losses in superconductors. The most direct is calorimetric, in which a superconducting coil is exposed to transient fields and the dissipated heat is measured by the boil-off of liquid helium. Another method is electrical, by measuring the phase angle between voltage and current. Wattmeters work on this principle.

The final methods are magnetic. Magnetization measurements are possible because magnetic moments are associated with circulating persistent surface currents and, in type-II superconductors in the mixed state, flux vortices. There are basically two types of magnetic methods. In the first, magnetization (magnetic moment per unit volume) is measured directly using, for example, a vibrating-sample magnetometer. Though lock-in detection at the frequency of vibration is used, this is a dc measurement, since the time required to cycle the field is on the order of 30 minutes. Measurements may be made while slowly ramping or stepping the field. The latter gives more accurate results if there is any imbalance in the pick-up coils.

In the second type of magnetic measurement, a sinusoidal ac field is applied (sometimes superimposed upon a dc field) and the derivative of the magnetization is detected by induction in a pickup coil. If the pickup coil is uncompensated, the induced voltage is proportional to the permeability  $\mu$ . If the coil is compensated (i.e., zero voltage when no sample is present), the induced voltage is proportional to the susceptibility  $\chi$ . In SI units,

$$\mu = \mu' - i\mu'' = \mu_0(1 + \chi) = \mu_0(1 + \chi' - i\chi''), \quad (1a)$$

$$\mu' = \mu_0(1 + \chi'), \quad (1b)$$

$$\mu'' = \mu_0\chi'', \quad (1c)$$

where single primes indicate the real (dispersive, inductive) components, the double primes indicate the imaginary (absorptive, resistive, loss) components, and  $\mu_0$  is the permeability of free space. The induced voltages may be integrated with respect to field (or with respect to time, since field is swept as a function of time) to yield the frequency-dependent magnetization.

The area enclosed by the dc or low-frequency ac hysteresis loop of magnetization vs. field is a direct measure of the hysteresis loss. Alternately, the imaginary component of susceptibility (or permeability) at low frequencies is an indirect measure of the hysteresis loss. This paper will discuss dc hysteresis loops and complex susceptibility. The commonly used method of integrated voltages will not be discussed. The conductor carries no transport current.

### Experimental Methods

DC hysteresis loops at about 4.1 K were obtained using a vibrating-sample magnetometer (VSM). Field values up to 1.6 MA/m (20 kOe) were determined from the current in a multifilamentary Nb-Ti superconducting magnet. No correction was made for trapped flux; zero-field-value errors are thus estimated to be  $\pm 4$  kA/m (50 Oe).

AC susceptibility was measured at 4 K with a lock-in amplifier and a compensated susceptometer of the type described in Ref. 2. If the induced waveform is nonsinusoidal, the lock-in amplifier will detect only the fundamental-frequency component. Losses that appear as harmonics are not detected. Therefore, this method is most suitable for relatively small ac field amplitudes. For very small ac field amplitudes,  $\chi''$  is known to be about zero, and this fact is used to adjust the phase  $\phi$  on the lock-in amplifier:

$$\chi' = |\chi| \cos \phi, \quad (2a)$$

$$\chi'' = |\chi| \sin \phi. \quad (2b)$$

The phase setting was kept constant for all fields, but was readjusted for each frequency. The background signal in the absence of a sample was subtracted from all measurements. The susceptometer was positioned in the bore of the same superconducting magnet as used with the VSM. Both apparatus were computer controlled. Magnetization and susceptibility accuracies are estimated to be within 5%.

The sample consisted of an insulated, Nb-Ti wire, cut into 14 straight segments 1.5 cm long, and bundled together. At low frequencies and for short samples (or short twist pitch), the filaments may be taken to be uncoupled. The field and all measurements were along the longitudinal axis. Before each set of measurements was made, the sample was warmed to above its critical temperature and then cooled in zero field. Demagnetization-factor corrections were negligible; the internal field was taken to be the same as the external applied

Contribution of the National Bureau of Standards, not subject to copyright.

Manuscript received September 10, 1984.

field. Magnetization and susceptibility were calculated per volume of superconductor filaments. Mass and volume measurements were made on a length of the wire, before and after dissolving the Cu matrix in  $\text{HNO}_3$ , to experimentally determine the filament radius and the volume and density of NbTi. The characteristics of the wire are given in Table I.<sup>3</sup>

#### AC Field Dependence of Complex Susceptibility

The ac susceptibility of the sample was measured for a few field amplitudes and frequencies as the dc bias field was stepped. Figures 1a-e show a comparison of the results. Only three branches are shown for each case to avoid redundancy. The shapes of the  $\chi'$  and  $\chi''$  curves are dependent upon both field amplitude and frequency. The frequency dependence is small, which is evidence that hysteresis is the major loss mechanism. For the smaller field amplitudes there are large differences between ascending and descending branches, and the branches are not symmetrical for positive and negative external dc fields (Figs. 1a-c). These effects may be attributed to relatively large filament-surface losses when the ac field is small. Bussière and Clem<sup>4</sup> discuss the applicable case when losses are associated with the bending of vortices trapped at a high angle to the surface, and the field is much less than the lower critical field  $H_{c1}$ . Short samples facilitate this effect.

Table I. Characteristics of NBS SRM 1457

Number of filaments:	180
Filament radius:	12.20 $\mu\text{m}$
Copper-to-NbTi volume ratio:	1.456
Density of NbTi alloy:	6.004 $\text{g/cm}^3$
NbTi-to-insulated-wire mass ratio:	0.3025

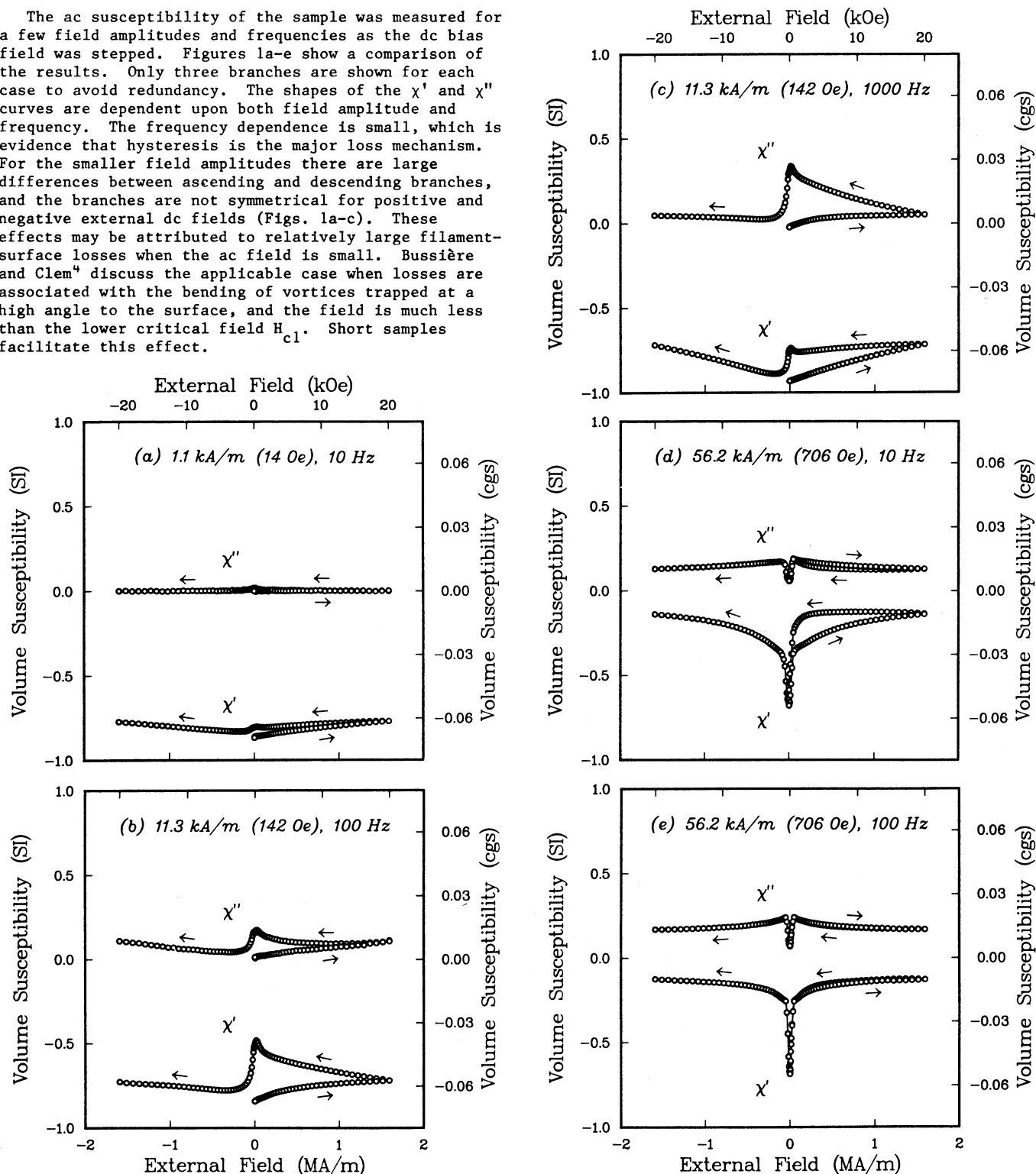


Figure 1. Imaginary ( $\chi''$ ) and real ( $\chi'$ ) components of ac susceptibility as a function of applied longitudinal dc field at 4 K. AC field amplitudes and frequencies are shown.

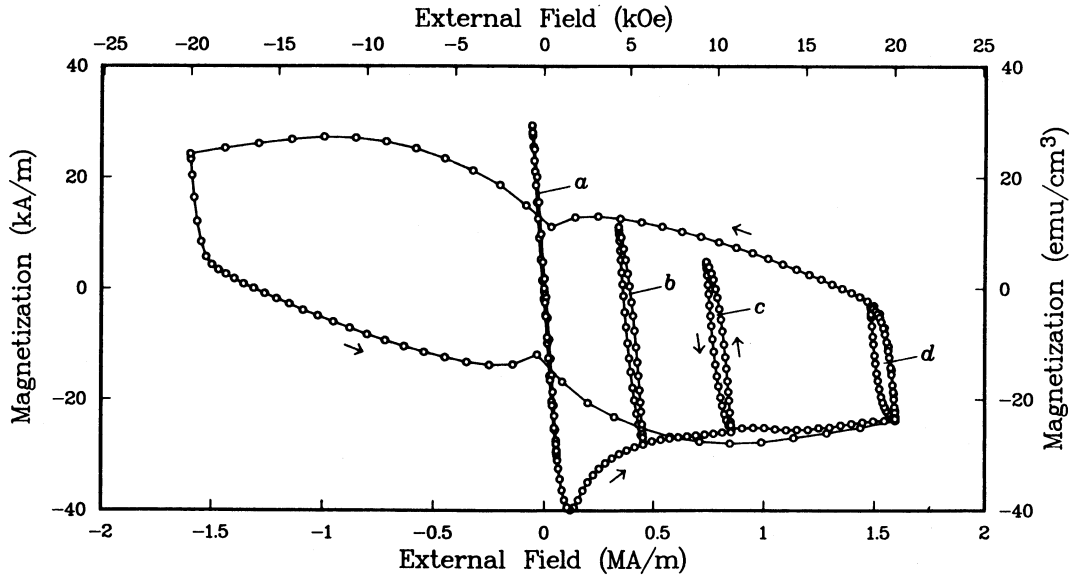


Figure 2. Magnetization  $M$  vs. dc field  $H$  at 4.1 K obtained with a VSM. The initial branch for zero trapped flux and four minor loops (a-d) are shown.

#### Theoretical Derivation of Complex Susceptibility

The following theoretical description of complex susceptibility is based on the development by Clem for the case of bulk-pinning hysteretic losses in type-II superconductors.<sup>5</sup> The model applies when the ac field amplitude is small and the field equations can be linearized. It will be shown that the dc hysteresis loop and the field dependence of the critical current density are predictive of the ac susceptibility.

The critical current as a function of transverse field<sup>6</sup> for the sample was converted to critical current density  $J_c$  using the total superconductor cross-sectional area (not including matrix material). A good fit was obtained to the Kim equation,

$$J_c(H) = J_c(0)/(1+H/H_0), \quad (3)$$

for fields  $H$  up to 4.8 MA/m (60 kOe). The adjustable parameters  $J_c(0)$  and  $H_0$  were found to be 9.2 GA/m<sup>2</sup> and 1.1 MA/m (14 kOe), respectively. While the longitudinal-field  $J_c$  is larger than the transverse-field  $J_c$ , they are, of course, identical at zero field.

The full-penetration longitudinal field  $H_p$  is a function of  $H$  owing to the field dependence<sup>6</sup> of  $J_c$ :

$$H_p(H) = J_c r, \quad (4)$$

where  $r$  is the filament radius. It is useful to define a parameter  $x$  as

$$x(H) = h/H_p = h/J_c r, \quad (5)$$

where  $h$  is the peak amplitude of the ac field that is superimposed upon  $H$ .

As shown by Clem and using Eqs. 1, the complex susceptibility may be expressed in terms of an idealized differential susceptibility for type-II superconductors  $\chi_{rev}$ :

$$\chi' = (1+\chi_{rev})g_1(x)-1, \quad (6)$$

$$\chi'' = (1+\chi_{rev})g_2(x), \quad (7)$$

where

$$\chi_{rev} = dM_{rev}/dH \quad (8)$$

where  $M_{rev}$  is the reversible magnetization, and

$$g_1(x) = x-5x^2/16, \quad 0 < x < 1, \quad (9a)$$

$$g_1(x) = [(-1+x-5x^2/16)\theta + (-4/3x+2-7x/4+13x^2/24)\sin\theta + (-1/2+x/2-x^2/6)\sin 2\theta + (-x/12+x^2/24)\sin 3\theta + (-x^2/192)\sin 4\theta]/\pi + 1, \quad x > 1, \quad (9b)$$

where  $\theta(x) = 2\sin^{-1}(x^{-1/2})$ ,  $\theta(1) = \pi$ ,  $\theta(\infty) = 0$ , and

$$g_2(x) = (4x-2x^2)/3\pi, \quad 0 < x < 1, \quad (10a)$$

$$g_2(x) = (4/x-2/x^2)/3\pi, \quad x > 1. \quad (10b)$$

Using Eqs. 6 and 7,  $\chi'$  and  $\chi''$  will be calculated for the sample. The major hysteresis loop for the sample is shown in Fig. 2. The lower critical field  $H_{c1}$  is

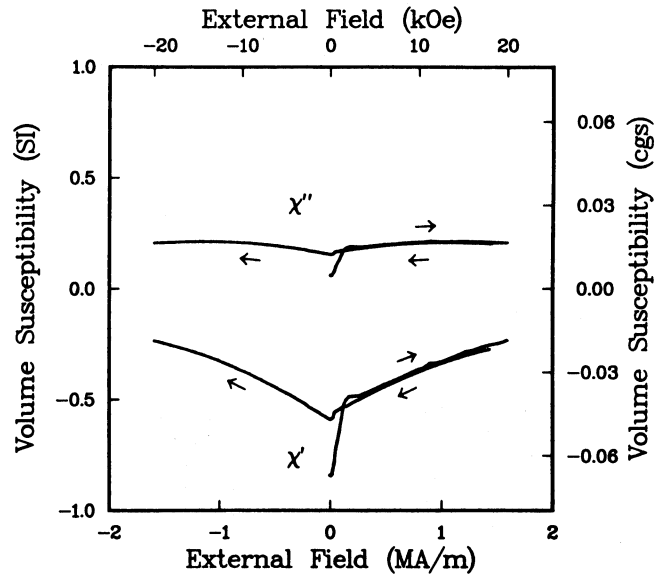


Figure 3. Imaginary ( $\chi''$ ) and real ( $\chi'$ ) components of ac susceptibility calculated for an ac field amplitude of 56.2 kA/m (706 Oe) using the theoretical model, the data in Fig. 2, and the field dependence of  $J_c$  (Eq. 3).

Table II. Comparison of hysteretic losses obtained by dc and ac methods for a field amplitude of 56.2 kA/m (706 Oe).

Center field (kA/m) (kOe)	Loss from minor- loop area (kJ/m <sup>3</sup> )	Loss from $\chi''$ Eq. 11 (kJ/m <sup>3</sup> )	Loss from Eqs. 12, 13 (kJ/m <sup>3</sup> )
0 0	0.6	0.7	0.9
400 5.0	1.3	2.0	2.1
800 10.0	1.4	1.8	2.6
1540 19.3	1.3	1.6	2.6

about 0.12 MA/m (1.5 kOe). The tangent to the curve at any H is the differential susceptibility  $\chi_{dc}$ . As an approximation,  $\chi_{dc}$  will be used for  $\chi_{rev}$ . This is somewhat reasonable for the initial branch of the hysteresis loop, but rather unreasonable for the later irreversible branches. However, theoretical  $\chi_{rev}$  and experimental  $\chi_{dc}$  are both about zero for fields much larger than  $H_{c1}$  and therefore do not greatly affect the computation.

A program was written to compute, for each value of H and  $\chi_{dc}$ , the predicted J(H), H(H), x(H),  $g_1(x)$ ,  $g_2(x)$ ,  $\chi'(x)$ , and  $\chi''(x)$ , given  $r^p$  and h. For  $h = 56.2$  kA/m (706 Oe),  $\chi'$  and  $\chi''$  as computed are plotted as a function of H in Fig. 3. As in Fig. 1, only the first three branches are shown. No adjustable parameters were used. A comparison with actual measured  $\chi'$  and  $\chi''$  in Figs. 1d,e shows good agreement in both shape and magnitude. Ideally, the computed curves in Fig. 3 would be symmetrical with respect to the external dc field and show no difference between the initial segment and the return portion, as expected from critical state theory.<sup>5</sup> Deviations from this are because  $\chi_{dc}$  was used instead of  $\chi_{rev}$ .

#### Hysteresis Loss

In this section, the minor loops in Fig. 2 are examined. The loss corresponding to each is calculated in three ways: minor-loop area, from  $\chi''$ , and from  $J_c$ .

The energy loss per unit volume per cycle is<sup>5</sup>

$$W = \pi \mu_0 h^2 \chi'' \quad (11)$$

Substituting for  $\chi''$  using Eqs. 7, 10b, and 5 for full field penetration ( $x > 1$ ),

$$W = (1 + \chi_{rev}) (4 \mu_0 h J_c r / 3) (1 - J_c r / 2h) \quad (12)$$

Except for the factor  $(1 + \chi_{rev})$ , the same equation is derived, in cgs emu, by Carr.<sup>7</sup> But for  $H \gg H_{c1}$ ,  $\chi_{rev} \approx 0$ . For partial field penetration ( $x < 1$ ),<sup>1</sup> using Eqs. 7, 10a, and 5, Eq. 11 may be expressed as

$$W = (1 + \chi_{rev}) (4 \mu_0 h^3 / 3 J_c r) (1 - h / 2 J_c r), \quad (13)$$

again similar to Carr's expression for this case.

Figure 2 shows four minor dc hysteresis loops for the sample determined experimentally with the VSM. The peak amplitude for each minor loop is 56.2 kA/m (706 Oe). The area enclosed by each loop was calculated numerically by

$$W = \mu_0 \oint H dM \approx \mu_0 \oint M dH. \quad (14)$$

This hysteresis loss is compared in Table II to the losses derived from Eq. 11, using  $\chi''$  measured at 10 Hz in 56.2 kA/m (706 Oe) peak field (Fig. 1d). Another comparison can be made with losses obtained using Eqs. 12 and 13, with  $J_c$  (at the center field) from Eq. 3. For the first minor loop,  $x < 1$ . Once again,  $\chi_{rev}$  is approximated by  $\chi_{dc}$  from the initial branch of the hysteresis loop. The agreement is reasonable, indicating that hysteretic losses may be measured directly with a hysteresis loop, or estimated by measurement of the imaginary component of low-frequency ac susceptibility, or from a reasonable estimate of  $J_c(H)$ .

Possible inaccuracies owing to the following should be considered: (1)  $J_c(H)$  was measured in transverse rather than longitudinal field; (2) losses are not entirely hysteretic; (3) induced voltage in susceptometer pickup coil contains higher-order harmonics; (4) applied ac field amplitude was not small enough to allow linearized field equations. Only the first of these is believed to be of significance, affecting the data in the last column of Table II.

#### Conclusion

The technique used to measure hysteretic losses might depend on one's application. If a field is stepped slowly, a dc hysteresis loop is obtained. If an alternating field is swept and the induced voltage integrated, an ac hysteresis loop may be obtained. For the general case, a dc bias field may be superimposed upon the stepped or alternating field. If the induced voltage is not integrated, but separated into real and imaginary parts, the complex susceptibility is obtained. Often, an ac susceptibility measurement is a convenient method. In this paper, it was shown that the complex susceptibility in an ac field could be reasonably predicted from the dc hysteresis loop, the critical current density, and the filament radius. Hysteresis losses obtained directly (Eq. 14) were compared to those obtained indirectly using experimental measurements of  $\chi''$  (Eq. 11) and average values of  $J_c$  and  $\chi_{dc}$  (Eqs. 12 and 13).

#### Acknowledgments

The authors are grateful to J. R. Clem for critical comments on an earlier draft of the manuscript. This work was sponsored by the Air Force Office of Scientific Research.

#### References and Footnotes

1. W. A. Fietz, "Electronic Integration Technique for Measuring Magnetization of Hysteretic Superconducting Materials," Rev. Sci. Instrum. 36, pp. 1621-26 (1965).
2. R. B. Goldfarb and J. V. Minervini, "Calibration of AC Susceptometer for Cylindrical Specimens," Rev. Sci. Instrum. 55, pp. 761-64 (1984).
3. NbTi wire, Standard Reference Material 1457 for critical current measurements, available from Office of Standard Reference Materials, National Bureau of Standards, Gaithersburg, MD 20899. The data on this wire in Table I are not certified by NBS.
4. J. F. Bussière and J. R. Clem, "Effect of trapped magnetic flux on ac losses of Nb<sub>3</sub>Sn," IEEE Trans. Magn. MAG-15, pp. 264-67 (1979).
5. J. R. Clem, "AC Losses in Type-II Superconductors," Ames Lab. Tech. Rept. IS-M 280, 1979.
6. Critical current was measured at 4 K by L. F. Goodrich using a transport current technique with a 0.2  $\mu$ V/cm criterion. The self-field contribution was not included. The demagnetization field, which would correct values of applied field, is about 0.6% at 1.6 MA/m (20 kOe) and 0.2% at 4.8 MA/m (60 kOe).
7. W. J. Carr, Jr., AC Loss and Macroscopic Theory of Superconductors, New York: Gordon and Breach, 1983, p. 70.